ELSEVIER

Journal of Organometallic Chemistry 542 (1997) 227–233

Journal of Organo metallic Chemistry

Synthesis and NMR spectroscopy of $[PtH_3(triphos)]^+$ and $[Pt(AuPPh_3)_3(triphos)]^+$

Crystal structure of $[Pt(AuPPh_3)_3(triphos)]^+$ (triphos $= CH_3C(CH_2PPh_2)_3$) [1]

Martin Peter [a], Helmuth Wachtler [a], Ernst Ellmerer-Müller [b], Karl-Hans Ongania [b],
Klaus Wurst [a], Paul Peringer [a,*]

[a] *Institut für Allgemeine, Anorganische und Theoretische Chemie, Universität Innsbruck, Innrain 52a, A-6020 Innsbruck, Austria*
[b] *Institut für Organische Chemie, Universität Innsbruck, Innrain 52a, A-6020 Innsbruck, Austria*

Received 26 October 1996; revised 5 February 1997

Abstract

The platinum(IV) complex $[PtH_3(triphos)]^+$ (**1**) is formed upon treatment of $[PtCl_2(triphos\text{-}P,P')]$ with $NaBH_4$. The complex **1** reacts with 3 equiv. of $[AuCl(PPh_3)]$ to give the tetrahedral $PtAu_3$ cluster $[Pt(triphos)(AuPPh_3)_3]^+$ (**2**). The complexes **1** and **2** are characterised by one- and two-dimensional multinuclear NMR spectroscopy. The platinum atom of **2** is bonded to the three phosphorus atoms of the triphos ligand and to three gold atoms giving a six-coordinate Pt atom. The cation has a crystallographically imposed threefold axis defined by the Pt atom and the centre of the Au_3 triangle. Some distances and angles: Au–Au 285.80(8), Pt–Au 262.99(8) pm, Au–P 226.9(3) pm, Pt–P 231.2(3), Au–Au–Pt 57.088(13)°, Au–Pt–Au 65.82(2)°. © 1997 Elsevier Science S.A.

1. Introduction

Venanzi and coworkers reported on a series of heterometallic tetrahedral MAu_3 clusters, in which triangular $[Au(PPh_3)]_3$ fragments are held together by polyhydride complexes of platinum group metals of the composition $[M(triphos)H_n]^{2+}$, e.g. $[Ir(triphos)H_2]^{2+}$, $[Rh(triphos)H_2]^{2+}$ and $[Ru(triphos)H_3]^{2+}$ [1–3]. In this paper we report, that treatment of the platinum(IV) complex $[PtH_3(triphos)]^+$ (**1**) with $[AuClPPh_3]$ results in the 'hydride-free' cluster $[Pt(triphos)(AuPPh_3)_3]^+$ (**2**). The new complexes **1** and **2** are characterised by multinuclear NMR spectroscopy, and **2** also by X-ray single crystal structure analysis. The related metallatetrahedrane clusters $[V(CO)_5(AuPPh_3)_3]$, $[ReH_3(PMe_2Ph)_3(AuPPh_3)_3]^+$, $[W(PMe_3)_3H_4(AuPPh_3)_3]^+$, $[RhH(CO)(PPh_3)_2(AuPPh_3)_3]^+$ and $[Co(CO)_3(AuPPh_3)_3]$ have been reported [4–8].

Platinum–gold clusters are known involving Pt:Au ratios of 6:1 to 1:9 [9–24]. There is one '$PtAu_3$' complex, $[Pt(PPh_3)_2(AuPPh_3)_3]^+$, which has been synthesised by the reaction of $[PtI(PPh_3)(AuPPh_3)_4]^+$ with PPh_3 [21].

2. Results and discussion

2.1. *Synthesis and NMR spectroscopic characterisation of $[PtH_3(triphos)]^+$ (1)*

The hydride complex **1** is formed in quantitative yield upon treatment of $[PtCl_2(triphos\text{-}P,P')]$ [25] with $NaBH_4$ in MeOH or MeOH–CH_2Cl_2 as shown in Eq. (1).

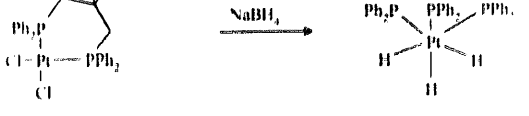

(1)

Solutions of **1** in these solvents decompose over ca. 1 day to uncharacterised products. The hydride **1** was

---

[*] Corresponding author.

[1] Dedicated to Professor K.E. Schwarzhans on the occasion of his 60th birthday.

0022-328X/97/$17.00 © 1997 Elsevier Science S.A. All rights reserved.
PII S0022-328X(97)00153-8

isolated as the BPh_4^- salt, which is soluble in CH_2Cl_2. Solutions of the tetraphenylborate in CH_2Cl_2 are stable when stabilised by a trace of HBF_4 in Et_2O. Interestingly, the platinum(IV) complex **1** is formed by reaction of a platinum(II) complex with the reducing reagent $NaBH_4$. We suggest that $[PtH_2(triphos\text{-}P,P')]$ is formed as intermediate and that subsequent oxidative addition of MeOH produces **1**. A similar reaction appears to have occurred during the treatment of $[Pt(C_6H_5)(MeOH)L_2]^+$ ($L = PMe_3$ or PEt_3) with $NaBH_4$ in MeOH where $[PtH_3(C_6H_5)L_2]^+$ was occasionally identified as an unstable by-product [26].

The PtP_3H_3 kernel of **1** is directly derived from one bond $\{^1H\}^{31}P^{195}Pt$ (Fig. 1) and $\{^{31}P\}^1H^{195}Pt$ shift correlation experiments, showing that three equivalent phosphorus and three equivalent hydrogen donor atoms are bound to the platinum atom. This is in keeping with the fac geometry of **1**, which is imposed by the triphos ligand. In a one bond $^1H^{195}Pt$ shift correlation experiment (Fig. 2), the tilt due to the passive $^{31}P-^1H$ and $^{195}Pt-^{31}P$ coupling indicates the same signs of the coupling constants, whereas in a one bond $^{31}P^{195}Pt$ shift correlation experiment, the tilt due to the passive $^{31}P-^1H$ and $^{195}Pt-^1H$ coupling indicates the reverse relative sign of the coupling constants. Values of ^1H, ^{31}P and ^{195}Pt NMR chemical shifts and coupling constants are given in Section 3.

2.2. Synthesis of $[Pt(triphos)(AuPPh_3)_3]^+$ (2)

The complex **2** is obtained by an almost quantitative reaction of **1** with 3 equiv. of $[AuCl(PPh_3)]$ in CH_2Cl_2–MeOH (Eq. (2)), and was isolated as chloride in good yields.

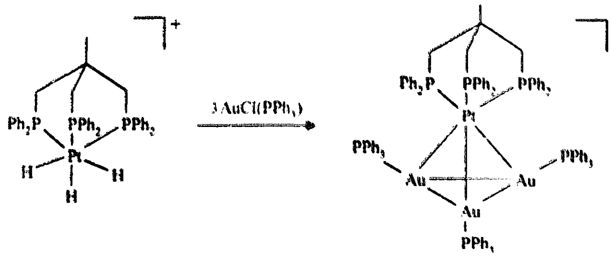

(2)

It is interesting to note, that while the formation of the clusters $[MH_2(triphos)(AuPPh_3)_3]^{2+}$, M = Rh, Ir, and

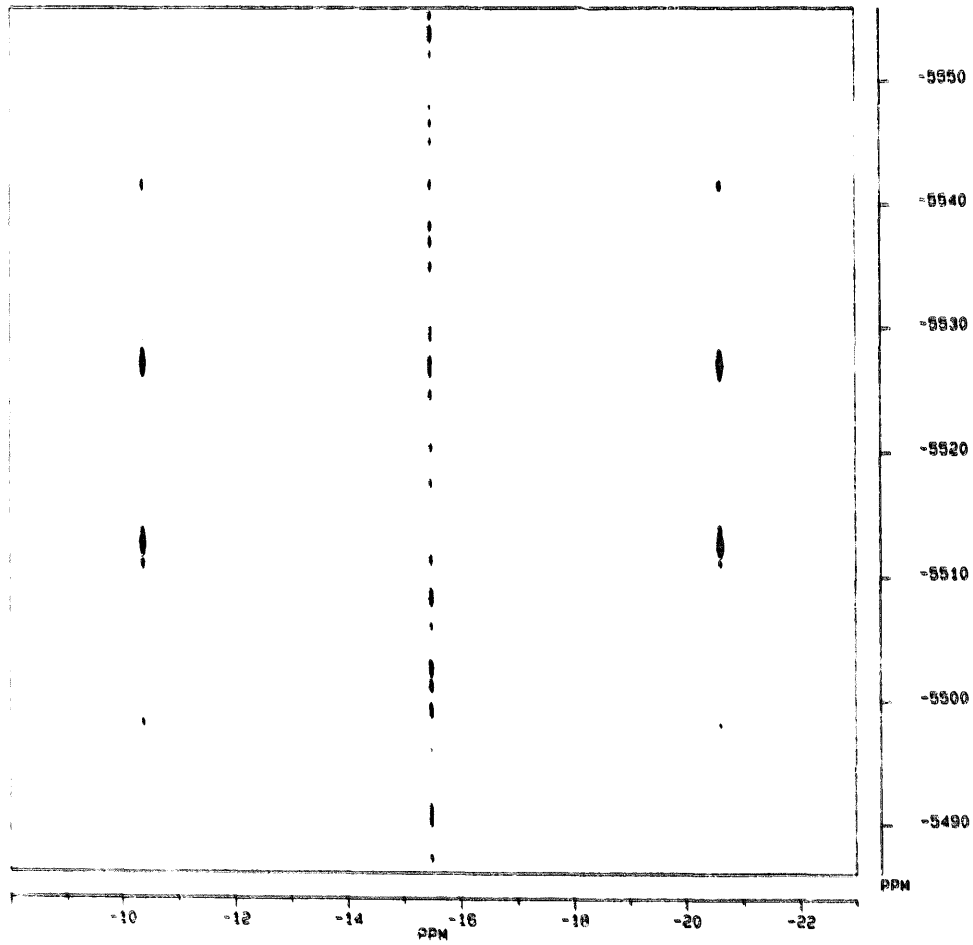

Fig. 1. One bond $\{^1H\}^{31}P^{195}Pt$ shift correlation experiment of **1** showing the $^{195}Pt-^1H$ coupling pattern in the δ ^{195}Pt direction (vertical) and the $^{195}Pt-^{31}P$ coupling in the δ ^{31}P direction (horizontal). The central vertical pattern is due to T_1 noise.

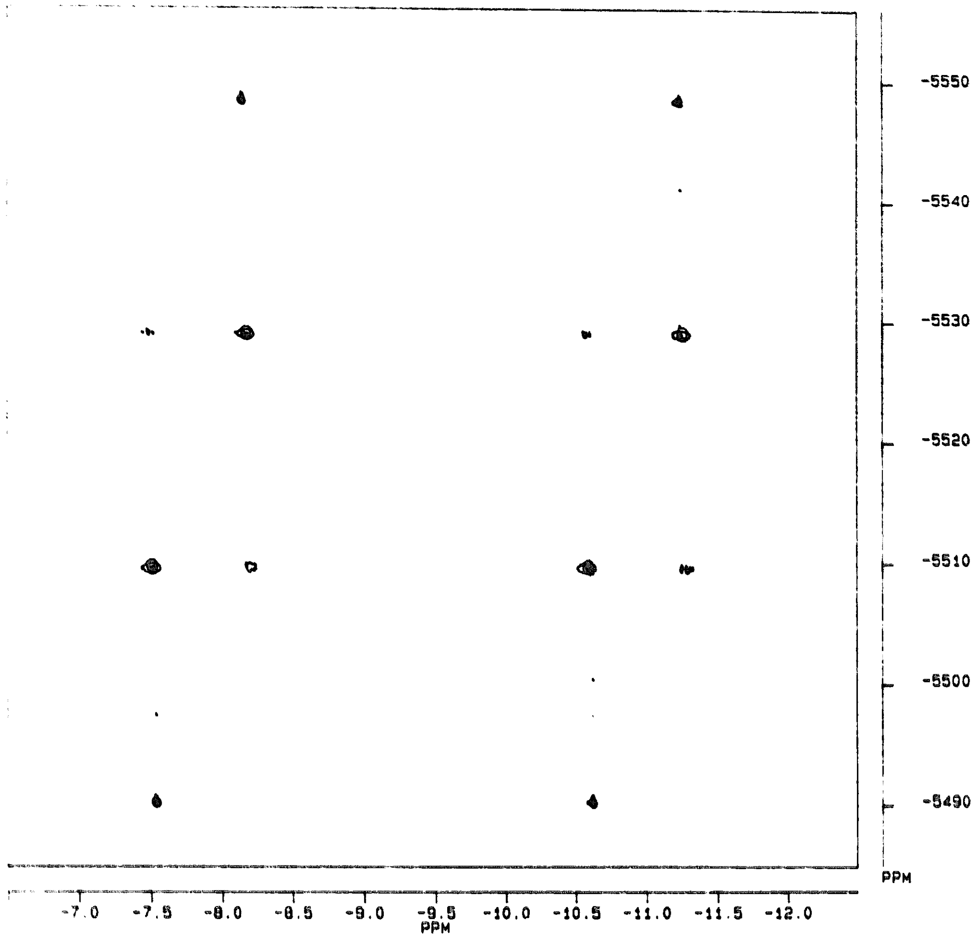

Fig. 2. One bond $^1H^{195}Pt$ shift correlation experiment of **1** showing the $^{195}Pt-^{31}P$ coupling pattern in the δ ^{195}Pt direction (vertical) and the $^{195}Pt-^1H$ coupling pattern in the δ ^{31}P direction (horizontal).

$[RuH_3(triphos)(AuPPh_3)_3]^{2+}$ [1–3] required the absence of chloride, in the case of **2** the reaction is carried out without removing chloride. The cluster **2** is also formed from $[Pt(triphos)PPh_3]$ [25,27] and $[AuCl(PPh_3)]$ besides other products.

As indicated in Section 2.4, there is no evidence for the presence of hydride ligands.

2.3. X-ray structure of $[Pt(triphos)(AuPPh_3)_3]^+$ (2)

The structure of **2** was determined by single crystal structure analysis and is presented in Fig. 3. Crystal and X-ray analytical data are shown in Table 1, fractional atomic coordinates in Table 2. The cluster **2** crystallises in the space group *R3c*. The same space group with very similar cell constants has been observed for the hydride clusters $[RhH_2(triphos)(AuPPh_3)_3](O_3SCF_3)_2$ [1] and $[RuH_3(triphos)(AuPPh_3)_3](PF_6)_2$ [3]. This indicates that the crystal packing is dominated by the large cations and that the remaining space (see Section 3) accommodates different types and numbers of anion and solvent of crystallisation. The complex **2** contains a $PtAu_3$ tetrahedron. The platinum atom is bonded to the three phosphorus atoms of the triphos ligand and to three gold atoms giving a six-coordinate Pt atom. Each Au atom is coordinated by one PPh_3 ligand. The cluster cation possesses a crystallographically imposed threefold axis defined by the Pt atom and the centre of the Au_3 triangle. The distances Pt–Au, Au–Au, Pt–P and Au–P and various angles are compared in Table 3 with the corresponding values of the compounds $[MHn(triphos)(AuPPh_3)_3]^{2+}$, M = Rh [1], Ir [2], *n* = 2; M = Ru [3], *n* = 3 and of $[V(CO)_5(AuPPh_3)_3]$ [4], $[ReH_3(PMe_2Ph)_3(AuPPh_3)_3]^+$ [5], $[W(PMe_3)_3H_4(AuPPh_3)_3]^+$ [6], $[RhH(CO)(PPh_3)_2(AuPPh_3)_3]^+$ [7] and $[Co(CO)_3(AuPPh_3)_3]$ [8]. The crystal structure of $[Pt(PPh_3)_2(AuPPh_3)_3]^+$ [21] has not been determined. The angles Au–Au–Pt and Au–Pt–Au are 57.088(13)° and 65.82(2)° respectively. The dihedral angle P1–Pt–Au–P2 amounts to 8.17(27)°, i.e. the orientation of the Pt(triphos) fragment relative to the Au_3 triangle is nearly eclipsed. The corresponding dihedral angles of $[MH_n(triphos)(AuPPh_3)_3]^{2+}$, M = Rh, Ru are 15.1° and 34.9° respectively [1,3].

2.4. NMR spectroscopy of [Pt(triphos)(AuPPh$_3$)$_3$]$^+$ (2)

We were unable to detect hydride signals by ^{1}H NMR spectroscopy between ambient temperature and 223 K.

The ^{31}P{^{1}H} NMR spectrum of the isotopomer without ^{195}Pt nuclei of 2 in CD_2Cl_2 at 297 K showed patterns consistent with an A_3B_3 spin system, which was simulated using the parameters given in Section 3. The resonances A and B are readily assigned to the PPh$_3$ and triphos ligands according to the size of the Pt–P coupling constants. Upon cooling of a CD_2Cl_2 solution down to 223 K, the inner signals of the quartet-like patterns broaden. The temperature dependence of the ^{31}P NMR spectra is compatible with a rotation of the [AuPPh$_3$]$_3$ moiety relative to the [Pt(triphos)] unit around the threefold axis. At ambient temperature the exchange process proceeds fast on the NMR time scale, whereas the slow exchange limit could not be reached due to solubility problems. Analogous dynamic processes were reported for the hydride clusters [MH$_2$(triphos)(AuPPh$_3$)$_3$], M = Rh, Ir, and [RuH$_3$(triphos)(AuPPh$_3$)$_3$]$^{2+}$ [1–3]. A ^{31}P NMR spectrum of [IrH$_2$(triphos)(AuPPh$_3$)$_3$]$^{2+}$ consistent with the static structure could be observed using a solution cooled below 173 K [2]. Fluxional NMR behaviour is also observed with [Pt(PPh$_3$)$_2$(AuPPh$_3$)$_3$]$^+$ [21].

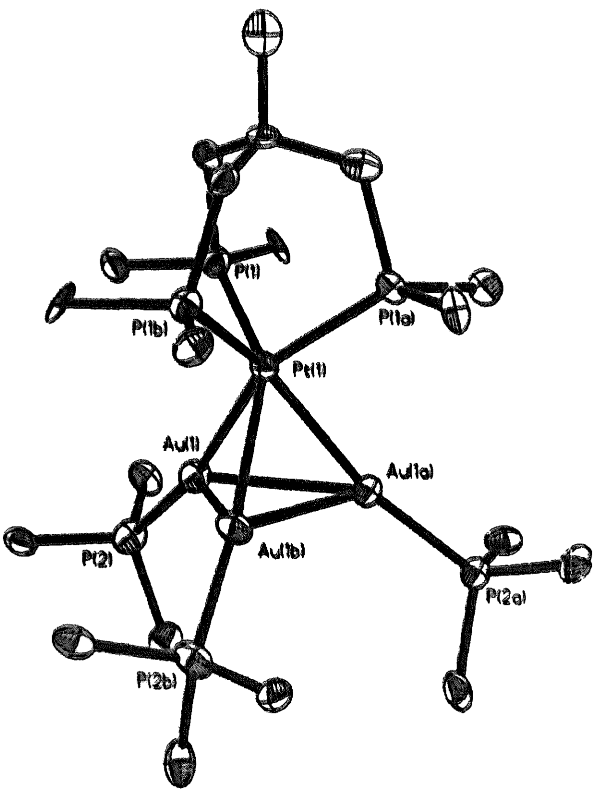

Fig. 3. View of the [Pt(triphos)(AuPPh$_3$)$_3$]$^+$ cation (2). For clarity, only the ipso carbon atoms of the phenyl groups are drawn.

Table 1
Crystal data and structure refinement for 2

Description	Value
Molecular formula	$C_{95}H_{84}Au_3ClP_6Pt \times 9CH_3OH$
Formula weight	2521.26
Crystal system	Trigonal
Space group	R3c (Nr. 161)
Unit cell dimensions	a = 2003.9(2) pm, α = 90° b = 2003.9(2) pm, β = 90° c = 4471.0(9) pm, γ = 120°
Volume	15.549(4) nm^3
Z	6
Temperature	213(2) K
Radiation	MoKα (λ = 71.073 pm)
Density (calculated)	1.616 Mg m^3
Absorption coefficient	5.750 mm^{-1}
$F(000)$	7428
Color, habit	Yellow column
Crystal size	0.5 × 0.25 × 0.22 mm
θ range for data collection	3.14 to 24.01°
Index ranges	$-22 \leq h \leq 22$, $-22 \leq k \leq 8$, $-2 \leq l \leq 51$
Reflections collected	5997
Independent reflections	2826 (R_{int} = 0.0524)
Reflections with $I > 2\sigma(I)$	2414
Absorption correction	ψ-scan
Max. and min. transmission	0.972 and 0.640
Refinement method	Full-matrix least-squares on F^2
Data/restraints/parameters	2826/1/351
Goodness-of-fit on F^2	1.039
Final R indices [$I > 2\sigma(I)$]	$R1$ = 0.0319, $wR2$ = 0.0559
R indices (all data)	$R1$ = 0.0462, $wR2$ = 0.0596
Absolute structure parameter	0.001(11)
Largest diff. peak and hole	723 and −802 e nm^{-3}
Data collection	
Diffractometer used	Siemens P4
Monochromator	Highly oriented graphite crystal
Scan type	ω
Scan speed	Variable; 6.0–35.0° min^{-1} in ω
Scan range (ω)	0.7°
Standard reflections	3 measured every 97 reflections
Solution and refinement	
System used	SHELXS-86 (Sheldrick, 1990) SHELXS-86 (Sheldrick, 1993)
Solution	Direct methods
Weighting scheme	Calc. $w = 1/[\sigma^2(F_o^2) + (0.0178P)^2 + 0.0000P]$ where $P = (F_o^2 + 2F_c^2)/3$
Hydrogen atoms	Calc., with isotropic displacement parameters 1.2 and 1.5 times higher than U_{eq} of the C atoms

2.5. Mass spectrometry of [Pt(triphos)(AuPPh$_3$)$_3$]$^+$ (2)

Gentle ionisation techniques such as fast atom bombardment (FAB) and plasma desorption (PD) have recently been applied to the study of metal cluster compounds [28].

The FAB technique has been used successfully to characterise the cluster 2. The highest mass seen is m/z

Table 2
Selected atomic coordinates ($\times 10^4$) and equivalent isotropic displacement parameters (pm$^2 \times 10^{-1}$) for **2**

	x	y	z	U_{eq}
Au(1)	9237(1)	10110(1)	8773(1)	24(1)
Pt(1)	10000	10000	8315(1)	18(1)
P(1)	8928(2)	9741(2)	8034(1)	22(1)
P(2)	8386(2)	10174(2)	9089(1)	28(1)
C(11)	9253(7)	9995(6)	7640(2)	23(3)
C(12)	10000	10000	7539(4)	22(5)
C(13)	10000	10000	7198(5)	38(6)
C(111)	8124(7)	8751(7)	8035(3)	22(3)
C(121)	8369(7)	10242(7)	8081(3)	26(3)
C(211)	7381(7)	9466(8)	8979(3)	28(3)
C(221)	8444(7)	11107(7)	9089(3)	28(3)
C(231)	8446(7)	9929(7)	9483(3)	31(3)
Cl(1)	6667	13333	9116(4)	276(10)

U_{eq} is defined as one-third of the trace of the orthogonalised U_{ij} tensor.

2197. This is consistent with $[Pt(triphos)(AuPPh_3)_3]^+$ and shows that the counterion Cl^- is not desorbed with the cation. This is in keeping with recent results of Kubiak and coworkers, who observed $[Ni_3(\mu_3\text{-L})(\mu_3\text{-I})(dppm)_3]^{n+}$, $n = 1,2$, as parent peaks in the FAB spectra of the clusters $[Ni_3(\mu_3\text{-L})(\mu_3\text{-I})(dppm)_3]I_n$, $n = 1,2$ [28].

The peak at 2197 is the base peak. Prominent fragments are $[Pt(triphos)\ Au_3PPh_3]^+$ (13%), $[Pt(triphos)\ Au_3]^+$ (9%) and $[Pt(triphos)\ Au_2]^+$ (6%).

3. Experimental section

NMR spectra were recorded on Bruker AC 200 and AM 300 spectrometers. The ^{31}P and ^{195}Pt NMR data are referenced against external 85% H_3PO_4 and 1 M Na_2PtCl_6. The one bond $^1H^{195}Pt$ shift correlation experiments were recorded using the standard HMQC sequence [29] preceded by a BIRD pulse; optional ^{31}P decoupling during acquisition was performed using the GARP sequence [30] and a BSV 3 amplifier; spectra resulted from a 2048 × 4096 data matrix size, 12 scans per t_1 value, delay time between scans 0.5 s; shifted square sine bell windows were used in both t_1 and t_2. The one bond $^{31}P^{195}Pt$ shift correlation experiments were recorded using the standard HMQC sequence; the ^{195}Pt pulses were generated by a second PTS and amplified by BSV 3; optional ^1H decoupling during acquisition was performed using the WALTZ sequence; $\{^1H\}$ spectra resulted from a 512 × 4096 data matrix size, 32 scans per t_1 value, delay time between scans 0.5 s; ^1H coupled spectra resulted from a 512 × 4096 data matrix size, 128 scans per t_1 value, delay time between scans 0.5 s; shifted square sine bell windows were used in both t_1 and t_2.

Mass spectra were recorded on a Finnigan MAT 95 instrument with the FAB technique.

The complexes $[PtCl_2(triphos\text{-}P,P')]$ [25], $[Pt(triphos)PPh_3]$ [25,27] and $[AuCl(PPh_3)]$ [31] were prepared as described previously. Triphos was purchased from Strem Chemical Corp. Elemental analyses were performed by the Institut für Physikalische Chemie, Universität Wien.

All reactions were carried out in Schlenk glassware by using standard inert atmosphere techniques.

3.1. Synthesis of $[PtH(triphos)]^+$ (1)

A 44.6 mg sample of $[PtCl_2(triphos\text{-}P,P')]$ (0.05 mmol) was dissolved in $MeOH\text{–}CH_2Cl_2$, (0.5 + 0.5 ml), and treated with $NaBH_4$ (20 mg, 0.52 mmol),

Table 3
Selected distances (pm) of **2** and related clusters

Complex	Au–Au	M–Au	Au–P	M–P	Ref.
$[Pt(triphos)(AuPPh_3)_3]Cl$	285.80(8)	262.99(8)	226.9(3)	231.2(3)	this work
$[Ru(triphos)H_3(AuPPh_3)_3](PF_6)_2$	300.3(1)	267.9(2)	232.6(5)	233.0(5)	[3]
$[Rh(triphos)H_2(AuPPh_3)_3](CF_3SO_3)_2$	288.7(1)	269.5(2)	226.0(5)	231.3(5)	[1]
$[Ir(triphos)H_2(AuPPh_3)_3](PF_6)_2$	288.2(2)	269.3(3)	227(1)	229(9)	[2]
$[Re(PMe_2Ph)_3H_4(AuPPh_3)_3](OR)$	293.1(2)	272.3(1)	226.7(5)	239.1(5)	[5]
$[V(CO)_5(AuPPh_3)_3]$	276.8(0)	270.9(1)	229.1(2)		[4]
	282.8(0)	273.6(1)	229.9(2)		
	285.5(0)	275.6(1)	230.0(2)		
$[W(PMe_3)_3H_4(AuPPh_3)_3]Cl$	288.1(1)	280.6(1)	228.7(3)	243.5(4)	[6]
	285.8(1)	279.3(1)	229.2(4)	250.7(4)	
	279.6(1)	281.2(1)	228.4(4)	249.8(4)	
$[Co(CO)_3(AuPPh_3)_3]$	279.52(2)	252.3(2)	226.5(2)		[8]
	281.76(6)	254.0(2)	227.1(2)		
	285.14(6)	250.4(1)	226.7(3)		
$[Rh(CO)(PPh_3)_2H(AuPPh_3)_3](PF_6)$	288.9(2)	266.4(3)	227(1)	236(1)	[7]
	281.4(2)	264.0(3)	229(1)	242(1)	
	291.4(2)	272.2(3)	223(1)		

The reaction mixture was stirred for 30 min and the solvent was evaporated under reduced pressure. The residue was dissolved in MeOH (1 ml) and added to a solution of $NaBPh_4$ (17.1 mg, 0.05 mmol) in MeOH (0.2 ml). The precipitate was washed with MeOH (0.5 ml) and dissolved in CH_2Cl_2 (1 ml). The CH_2Cl_2 phase was evaporated under reduced pressure leaving the product as white powder in almost quantitative yield. Anal. Calcd. for $C_{65}H_{62}BP_3Pt \cdot 2.8CH_2Cl_2$ C, 59.0; H 4.94. Found C, 59.1; H, 4.72.

^{31}P NMR (81.015 MHz, CD_2Cl_2, 297 K): δ −15.5 (^1J(PtP) 1234 Hz); ^1H NMR (200.08 MHz, CD_2Cl_2): δ −9.4 (hydride, ^1J(Pt,H) 929 Hz, ^2J(P,H) ca. 195 Hz and ca. 7 Hz); δ 2.4 (d, CH_2, m, 6H, ^2J(P,H) 9 Hz); δ 1.2 (q, CH_3, m, 3H, ^4J(P,H) 3 Hz); ^{195}Pt NMR (43.022 MHz, CD_2Cl_2.): δ −5520.

3.2. Synthesis of $[Pt(triphos)(AuPPh_3)_3]^+$ (2)

0.05 mmol of $[PtH_3(triphos)]^+$ was prepared in situ as described above. $[AuCl(PPh_3)]$ (74.2 mg, 0.015 mmol) was added. The mixture was allowed to stand for 1 day and washed with H_2O (3 × 0.5 ml). The solvent was evaporated under reduced pressure and the residue was recrystallised by dissolving in MeOH (0.3 ml) and allowing to stand. Orange-red crystals deposit in ca. 65% yield. Found: C, 50.22; H, 4.01; Cl, 1.18. Calcd. for $C_{95}H_{84}Au_3ClP_6 \cdot 5MeOH$: C, 50.19; H, 4.38; Cl, 1.48. ^{31}P NMR (81.015 MHz, CD_2Cl_2, 297 K): δ 53.8 (PPh_3, m with ^{195}Pt satellites, ^3J(P,P) 52.3 Hz, ^2J(Pt,P) 296.7 Hz); δ 26.3 (triphos, m with ^{195}Pt satellites, ^2J(Pt,P) 2229 Hz); ^1H NMR (200.08 MHz, CD_2Cl_2, 297 K): δ 2.3 (CH_2, m, 6H), δ 1.2 (CH_3, m, 3H); ^{195}Pt NMR (43.022 MHz, CD_2Cl_2, 297 K): δ −5110 (qq).

3.3. Crystal structure determination

A column having approximate dimensions 0.5 × 0.25 × 0.22 mm^3 was mounted on a Siemens P4 diffractometer with a graphite-monochromatised Mo Kα radiation. The unit cell parameters were determined and refined from 22 randomly selected reflections, obtained by P4 automatic routines. Data were measured via ω-scans and corrected for Lorentz and polarisation effects. An empirical absorption correction [32] based on a series of ψ-scans was applied. A total of 5997 reflections were collected, of which 2826 were unique and 2414 with $I > 2\sigma(I)$. The structure was solved by direct methods (SHELXS-86) [33] and refined by a full matrix least squares procedure using F^2 (SHELXL-93) [34]. All non-hydrogen atoms of the cluster were refined with anisotropic displacement parameters. The hydrogen atoms of the phosphine ligands were included in the refinement at calculated positions using a riding model. The solvent molecules were refined with isotropic displacement parameters. One of the solvent molecules was found to be disordered and was refined in two positions with occupancy of 0.5.

After calculations by Kempster and Lipson [35] only 85% of space is filled. This could be reason for the large thermal motions of the solvent molecules and the chlorine anion. The chlorine anion lies at a crystallographic threefold axis with a large thermal motion perpendicular to the axis. A slight disordering around this axis, produced by the electrostatic field of the surrounding cations, can also be responsible for this motion.

References

[1] A. Albinati, F. Demartin, P. Janser, L.F. Rhodes, L.M. Venanzi, J. Am. Chem. Soc. 111 (1989) 2115.

[2] A. Albinati, J. Eckert, P. Hofmann, H. Rüegger, L.M. Venanzi, Inorg. Chem. 32 (1993) 2377.

[3] A. Albinati, L.M. Venanzi, G. Wang, Inorg. Chem. 32 (1993) 3660.

[4] J.E. Ellis, J. Am. Chem. Soc. 103 (1981) 6106.

[5] B.R. Sutherland, K. Folting, W.E. Streib, D.M. Ho, J.C. Huffman, K.G. Caulton, J. Am. Chem. Soc. 109 (1987) 3489.

[6] A. Berry, M.L.H. Green, J.A. Bandy, K. Prout, J. Chem. Soc. Dalton Trans. (1991) 2185.

[7] P.D. Boyle, B.J. Johnson, A. Buehler, L.H. Pignolet, Inorg. Chem. 25 (1986) 5.

[8] G. Beuter, A. Brodbeck, M. Holzer, S. Maier, J. Strähle, Z. Anorg. Allg. Chem. 616 (1992) 27.

[9] M.F.J. Schoondergang, J.J. Bour, G.P.F. van Strijdonck, P.P.J. Schlebos, W.P. Bosman, J.M.M. Smits, P.T. Beurskens, J.J. Steggerda, Inorg. Chem. 30 (1991) 2048.

[10] M. Peter, P. Peringer, E.P. Müller, J. Chem. Soc. Dalton Trans. (1991) 2459.

[11] J.J. Bour, R.P.F. Kanters, P.P.J. Schlebos, W.P. Bosman, H. Behm, P.T. Beurskens, J.J. Steggerda, Recl. Trav. Chim. Pays-Bas 106 (1987) 157.

[12] J.J. Bour, R.P.F. Kanters, P.P.J. Schlebos, J.J. Steggerda, Recl. Trav. Chim. Pays-Bas 107 (1988) 211.

[13] J.J. Bour, P.P.J. Schlebos, R.P.F. Kanters, M.F.J. Schoondergang, H. Addens, A. Overweg, J.J. Steggerda, Inorg. Chim. Acta 181 (1991' 195.

[14] R.P.F. Kanters, P.P.J. Schlebos, J.J. Bour, W.P. Bosman, H.J. Behm, J.J. Steggerda, Inorg. Chem. 27 (1988) 4034.

[15] D.E. Smith, A.J. Welch, I. Treurnicht, R.J. Puddephatt, Inorg. Chem. 25 (1986) 4616.

[16] A. Albinati, H. Lehner, L.M. Venanzi, M. Wolfer, Inorg. Chem. 26 (1987) 3933.

[17] T.G.M.M. Kappen, P.P.J. Schlebos, J.J. Bour, W.P. Bosman, G. Beurskens, J.M.M. Smits, P.T. Beurskens, J.J. Steggerda, Inorg. Chem. 34 (1995) 2121.

[18] T.G.M.M. Kappen, P.P.J. Schlebos, J.J. Bour, W.P. Bosman, G. Beurskens, J.M.M. Smits, P.T. Beurskens, J.J. Steggerda, Inorg. Chem. 34 (1995) 2133.

[19] P.D. Boyle, B.J. Johnson, B.D. Alexander, J.A. Casalnuovo, P.R. Gannon, S.M. Johnson, E.A. Larka, A.M. Mueting, L.H. Pignolet, Inorg. Chem. 26 (1987) 1346.

[20] L.N. Ito, J.D. Sweet, A.M. Mueting, L.H. Pignolet, M.F.J. Schoondergang, J.J. Steggerda, Inorg. Chem. 28 (1989) 3696.

[21] L.N. Ito, A.M.P. Felicissimo, L.H. Pignolet, Inorg. Chem. 30 (1991) 387.

[22] J.J. Bour, P.P.J. Schlebos, R.P.F. Kanters, W.P. Bosman, J.M.M. Smits, P.T. Beurskens, J.J. Steggerda, Inorg. Chim. Acta 171 (1990) 177.

[23] P. Braunstein, H. Lenner, D. Matt, A. Tiripicchio, M. Tiripicchio-Camellini, Angew. Chem. Int. Ed. Engl. 96 (1984) 304.

[24] M.F. Hallam, D.M.P. Mingos, T. Adatia, M. McPartlin, J. Chem. Soc. Dalton Trans. (1988) 335.

[25] J. Chatt, R. Mason, D.W. Meek, J. Am. Chem. Soc. 97 (1975) 3826.

[26] D.P. Arnold, M.A. Bennett, Inorg. Chem. 23 (1984) 2110.

[27] L.M. Green, Y. Park, D.W. Meek, Inorg. Chem. 27 (1988) 1658.

[28] D.A. Morgenstern, C.C. Bonham, A.P. Rothwell, K.V. Wood, C.P. Kubiak, Polyhedron 14 (1995) 1129.

[29] A. Bax, M.F. Summers, J. Am. Chem. Soc. 108 (1986) 2093.

[30] A.J. Shaka, P.B. Barker, D.J. Ruben, J. Magn. Reson. 98 (1982) 286.

[31] P. Braunstein, H. Lehner, D. Matt, Inorg. Synth. 27 (1990) 218.

[32] A.C.T. North, D. Phillips, F.S. Mathews, Acta Crystallogr. Sect. A: 24 (1968) 351.

[33] G.M. Sheldrick, SHELXS-86: Program for Crystal Structure Solutions, Göttingen, 1986.

[34] G.M. Sheldrick, SHELXL-93: Program for Refinement of Crystal Structures, Göttingen, 1993.

[35] D.T. Kemster, H. Lipson, Acta Crystallogr. Sect. B: 28 (1972) 3674.